FEB 20 1997
OSTI

CONF-961202--84

ANL/CMT/CP-90404

DISSOLUTION RATES OF DWPF GLASSES FROM LONG-TERM PCT

W. L. Ebert and S.-W. Tam

Chemical Technology Division
ARGONNE NATIONAL LABORATORY
9700 South Cass Avenue
Argonne, IL 60439-4837

The submitted manuscript has been authored by a contractor of the U.S. Government under contract No. W-31-108-ENG-38. Accordingly, the U.S. Government retains a nonexclusive, royalty-free license to publish or reproduce the published form of this contribution, or allow others to do so, for U.S. Government purposes.

MASTER

Accepted for Publication

1996 Fall Meeting
Materials Research Society
Boston, MA
December 2-5, 1996

DISTRIBUTION OF THIS DOCUMENT IS UNLIMITED

Work supported by the U.S. Department of Energy, Office of Environmental Management, under contract W-31-109-ENG-38.

DISCLAIMER

This report was prepared as an account of work sponsored by an agency of the United States Government. Neither the United States Government nor any agency thereof, nor any of their employees, make any warranty, express or implied, or assumes any legal liability or responsibility for the accuracy, completeness, or usefulness of any information, apparatus, product, or process disclosed, or represents that its use would not infringe privately owned rights. Reference herein to any specific commercial product, process, or service by trade name, trademark, manufacturer, or otherwise does not necessarily constitute or imply its endorsement, recommendation, or favoring by the United States Government or any agency thereof. The views and opinions of authors expressed herein do not necessarily state or reflect those of the United States Government or any agency thereof.

DISCLAIMER

Portions of this document may be illegible in electronic image products. Images are produced from the best available original document.

DISSOLUTION RATES OF DWPF GLASSES FROM LONG-TERM PCT

W. L. Ebert and S.-W. Tam
Chemical Technology Division, Argonne National Laboratory, Argonne, IL 60439

ABSTRACT

We have characterized the corrosion behavior of several Defense Waste Processing Facility (DWPF) reference waste glasses by conducting static dissolution tests with crushed glasses. Glass dissolution rates were calculated from measured B concentrations in tests conducted for up to five years. The dissolution rates of all glasses increased significantly after certain alteration phases precipitated. Calculation of the dissolution rates was complicated by the decrease in the available surface area as the glass dissolves. We took the loss of surface area into account by modeling the particles to be spheres, then extracting from the short-term test results the dissolution rate corresponding to a linear decrease in the radius of spherical particles. The measured extent of dissolution in tests conducted for longer times was less than predicted with this linear dissolution model. This indicates that advanced stages of corrosion are affected by another process besides dissolution, which we believe to be associated with a decrease in the precipitation rate of the alteration phases. These results show that the dissolution rate measured soon after the formation of certain alteration phases provides an upper limit for the long-term dissolution rate, and can be used to determine a bounding value for the source term for radionuclide release from waste glasses. The long-term dissolution rates measured in tests at 20,000 m^{-1} at 90°C in tuff groundwater at pH values near 12 are about 0.2, 0.07, and 0.04 $g/(m^2 \cdot d)$ for the Environmental Assessment glass and glasses made with SRL 131 and SRL 202 frits, respectively.

INTRODUCTION

We have conducted static dissolution tests to characterize the long-term corrosion behavior of several reference high-level waste glasses for the Defense Waste Processing Facility (DWPF). Many tests were conducted with crushed glass to characterize the dissolution behavior as the solution becomes highly concentrated in glass components. As has been observed with other glasses, after an initially high dissolution rate in dilute leachant solutions, the glass dissolution rate decreases to a very low value as the solution concentrations of glass components increase to apparent saturation values. However, the formation of certain alteration phases has been observed to cause a significant increase in the dissolution rates of many glasses [1-4]. The time required for these phases to form depends on the glass composition, temperature, and glass surface area/solution volume ratio (S/V) of the test, as well as the nucleation kinetics of the precipitated phases. For durable glasses, several years may be required before rate-affecting phases form under a particular set of test conditions, while such phases may form within a few months in similar tests with less durable glasses. The questions we address in this paper are whether the rate expression that has been determined from corrosion behavior prior to formation of rate-affecting alteration phases can also be used to calculate long-term corrosion behavior after they have formed, and whether the measured rate is likely to provide an upper bound to the long-term corrosion rate.

The observed effect of alteration phase formation on the glass dissolution rate is qualitatively consistent with the glass corrosion mechanism used to model long-term corrosion behavior [5-8]. Glass is thermodynamically unstable with respect to a suite of alteration phases; which phases form depends, in part, on the glass composition. Contact of a glass by water provides a kinetically favorable pathway for the transformation of glass to alteration phases via a dissolution-reprecipitation mechanism. As glass dissolves, a quasi-equilibrium between the glass and the solution is approached. This equilibrium is modeled as the hydrolysis of an $Si–OSi(OH)_3$ bond at the surface to release orthosilicic acid into solution. The net dissolution rate of the glass becomes very low as the solution approaches saturation with respect to chalcedony or other surrogates for the glass. The formation of some alteration phases provides a demand for silicon and affects the equilibrium between the glass and the solution such that the glass dissolution rate

increases. Of course, the solution concentrations of other components of the alteration phases will also affect phase formation and the resulting demand for silicon, as given in the equilibrium expression for each alteration phase. For example, the formation of analcime [$NaAlSi_2O_6 \cdot H_2O$] depends on the concentrations of Na, Al, and Si species, as well as the pH and temperature.

The effect of alteration phase formation on the glass dissolution rate will also depend on how fast the phases precipitate. Some Si-bearing phases may form very early in the reaction, but if their precipitation rates are lower than the glass dissolution rate, even under near-saturation conditions, the formation of those phases will not significantly affect the dissolution rate of the glass. For example, clays have been observed to form in tests with many glasses without measurably affecting the dissolution rate [9-11]. After longer reaction times, other phases may form at rates that are much higher than the glass dissolution rate. Formation of these phases may have a pronounced effect on the glass dissolution rate. For example, the formation of analcime has been observed to coincide with an increase in the dissolution rate of some glasses [1-3, 9-13], but may not affect the dissolution rates of others. The effect of alteration phase formation on the glass dissolution rate depends on the relative stabilities of the glass and the alteration phases [8].

The glass dissolution rate prior to the formation of alteration phases can be written as [14]

$$\text{rate} = k_0 10^{\eta pH} e^{-E_a/RT}\left[1-\left(\frac{Q}{K}\right)^{\sigma}\right] \qquad (1)$$

where k_0 is the intrinsic dissolution rate that depends only on the glass composition, η is the coefficient of the pH-dependence, E_a is the activation energy, Q is the ion activity product of the solution, K is the equilibrium constant for the hydrolysis reaction, and σ is the reaction order. The values of η, E_a, K, and σ have been measured to be about 0.4, 80 kJ/mol, $10^{-3.1}$, and 0.1, respectively, for DWPF glasses [15, 16]. In the case that the hydrolysis of an $Si\text{-}OSi(OH)_3$ bond at the glass surface is the rate-determining step, Q and K depend only on the activity of orthosilicic acid. The term in brackets is referred to as the affinity term, which may vary between values of 1 in highly dilute solutions to near 0 in nearly saturated solutions. This expression has been found to describe the corrosion behavior of many nuclear waste glasses well prior to the formation of alteration phases. The glass dissolution rate is usually measured experimentally based on the accumulation of B or other highly soluble glass component in the leachate solution. The goal of the present work is to determine if the rate expression in Eq. 1 also describes the corrosion behavior after phases form that increase the dissolution rate, or if additional terms are required.

Alteration phase formation may affect the pH and the value of Q. The other parameters depend on the glass composition. In the limit that the solution chemistry becomes fixed by an equilibrium between the solution and the alteration phases, the value of the affinity term will become constant. If the pH and temperature remain constant, then the glass dissolution rate will also be constant as long as the same suite of alteration phases controls the corrosion behavior. If the formation of alteration phases only affects the value of Q, then Eq. 1 predicts that the long-term dissolution rate will vary with the precipitation rate of the alteration phases. If phases precipitate much faster than the glass can dissolve, then glass dissolution is predicted to proceed at a constant rate. If the precipitation rate decreases, then Q will increase and the glass dissolution rate will decrease. Equation 1 describes glass dissolution, not the precipitation of alteration phases.

We have evaluated the results of long-term Product Consistency Tests (PCTs) to address the use of Eq. 1 to describe corrosion behavior after rate-controlling alteration phases have formed, and to determine if the glass dissolution rate becomes constant at advanced stages of corrosion. One complication of extracting dissolution rates from the results of tests with crushed glass is that the available surface area decreases appreciably as the glass dissolves. We have taken the loss of surface area into account by modeling the particles to be spheres, then extracting the value of a dissolution rate corresponding to a linear decrease in the radius with time. The change in NL(B) corresponding to this constant shrinkage rate was then compared to test results that were adjusted to take into account the decrease in the surface area with the same geometric model.

EXPERIMENTAL

Tests were conducted with crushed DWPF reference glasses of the size fraction -100 +200 mesh and tuff groundwater solutions [2, 3, 9, 10, 17, 18]. The leachant solutions used in the various tests were prepared by reacting groundwater from well J-13 with crushed tuff (<100 mesh) at 90°C for four weeks then passing the solution through a 100-nm filter. The resulting solution is referred to as EJ-13 water. Different batches of water were prepared for each series of tests. The concentrations of the major components are about 35-45 mg/L Si, 45-55 mg/L Na, and 120 mg/L HCO_3^-; the solution pH was near 8 (measured at room temperature). Tests were conducted at glass/leachant mass ratios of 1:10 and 1:1 to attain S/V of about 2000 and 20,000 m^{-1}, respectively. All tests were conducted in convection ovens set at 90°C. At the end of each test, the leachate was analyzed for pH and cation concentrations, and the reacted solids were analyzed. Details regarding phase identification, the disposition of radionuclides, etc. are provided in the above references.

RESULTS AND DISCUSSION

The compositions of the glasses discussed in this paper are given in Table I. The results of static dissolution tests conducted with these glasses are summarized in Table II. The test durations before and after rate-affecting alteration phases formed are listed in Table II. For example, rate-affecting alteration phases were detected in the 364-day test with SRL 202A at 20,000 m^{-1}, but not in the 182-day test. The alteration phases that formed coincident with the increase in the dissolution rate are also listed in Table II. For some glasses, rate-affecting alteration phases had only formed in the test with the longest duration or not enough data were available to determine the rate. In other tests, the glass had completely altered within the test interval in which the rate-affecting phases had formed. While the qualitative behavior observed in those tests is consistent with the effects of alteration phase formation seen in other tests, only lower bounds to the dissolution rates can be extracted. The results of those tests are not evaluated here.

The extent of reaction is commonly expressed in terms of the normalized mass loss, which is calculated by dividing the mass of a glass component in solution by the surface area of glass exposed in the test and by the mass fraction of that component in the glass. The normalized mass loss can be written either in terms of the mass, m_i, or the concentration, c_i, of an element in solution

$$NL(i) = \frac{\left(m_i - m_i^o\right)}{\left(S \bullet f_i\right)} = \frac{\left(c_i - c_i^o\right)}{\left([S/V] \bullet f_i\right)} \qquad (2)$$

where m_i° and c_i° are the mass and concentration of species i in the leachant solution, and f_i is the mass fraction of i in the glass. Note that NL(i) has the units of mass *glass* per area, not mass of i per area, because of the inclusion of the f_i term. Different values of NL(i) will be calculated for different i if glass dissolution is nonstoichiometric or if glass components become incorporated into alteration phases. The rate calculated based on the release of B is usually assumed to provide the best measure of the extent of glass dissolution, since B is highly soluble and is sensitive to the dissolution of the glass matrix.

While the accumulated amount of B is measured directly, the change in the surface area during the test must be estimated analytically. We have calculated NL(B) with the initial surface area and the surface area estimated to remain at the end of the test. The initial surface area was calculated by assuming the glass grains to be spheres having a diameter equal to the arithmetic

Table I. Compositions of Glasses

	SRL 131	SRL 202	SRL EA		SRL 131	SRL 202	SRL EA
Al_2O_3	3.27	3.84	3.60	NiO	1.24	0.82	0.53
Am_2O_3	0.0004[a]	0.0004[a]	—	Np_2O_3	0.009[a]	0.009[a]	—
B_2O_3	9.65	7.97	11.16	PbO	—	0.01	—
BaO	0.16	0.22	—	Pu_2O_3	0.009[a]	0.009[a]	—
CaO	0.93	1.20	1.23	SiO_2	43.8	48.9	48.76
Cr_2O_3	0.13	0.08	—	SrO	0.01	0.03	—
CuO	0.02	0.04	—	TcO_2	0.03	0.03	—
Fe_2O_3	12.7[b]	11.4 [b]	9.3 b	ThO_2	0.03	0.03	—
K_2O	3.86	3.71	0.04	TiO_2	0.65	0.91	0.65
Li_2O	3.00	4.23	4.21	U_3O_8	2.73	1.93	—
MgO	1.31	1.32	1.79	ZnO	0.02	0.02	0.26
MnO_2	2.43	2.21	1.36	ZrO_2	0.22	0.10	0.48
Na_2O	12.1	8.92	16.88	Total	98.3	98.6	100.25

[a]These radionuclides present in actinide-doped glasses, but not in non-doped glasses.
[b]All iron assumed to be Fe(III).

Table II. Summary of Test Results

Glass	S/V, m^{-1}	Time, days	pH	Alteration Phases[a]	Ref.
SRL 131A	2000	140-280	10.7-11.5	SMEC; ANAL; GYR; WEEK	17
SRL 131A	20,000	98-182	12.1-12.4	SMEC; ANAL; GYR; WEEK	17
SRL 131S[c]	2000	980-1800	11.7-12.0	SMEC; ANAL	2
SRL 131R[b]	2000	>1800[b]	11.9	SMEC	2
SRL 200S[d]	20,000	182-330	11.8-12.3	SMEC; ANAL; CLIN; GYR; WEEK	2
SRL 200R[b]	20,000	>1800[b]	11.7	SMEC	2
SRL 202U	20,000	182-364	11.5-11.7	SMEC; ANAL; GYR; WEEK	17
SRL 202A[c]	2000	1822	11.3	SMEC; ANAL; GYR; WEEK	17
SRL 202A	20,000	182-364	11.3-11.9	SMEC; ANAL; GYR; WEEK	17
SRL EA[d]	2000	313-369	11.8-12.1	SMEC; ANAL; GMEL; GYR; ZEO	18
SRL EA	20,000	<22[e]	12.0-12.4	SMEC; ANAL; GMEL; ZEO	18

[a]SMEC = smectite clay; ANAL = analcime; GYR = gyrolite or other Ca-silicate; WEEK = weeksite; ZEO = Na-Al-silicate phase; GMEL = gmelinite; CLIN = clinoptilolite.
[b]Rate-affecting alteration phases did not form within the longest time tested.
[c]Rate-affecting alteration phases only formed at the longest time tested.
[d]Too few data to extract rate.
[e]Rate-affecting phases formed within shortest time tested.

average of the sieve sizes. For -100 +200 mesh glass, the diameter was assumed to be 112 μm. The remaining surface area at the end of a test was calculated with Eq. 3 [14]:

$$S_t = \left(\frac{3\, m_o^{1/3} \left(m_o - \frac{m_B}{f_B} \right)^{2/3}}{(\rho r_o)} \right) \qquad (3)$$

where S_t is the surface area remaining at time t, m_o is the initial mass of glass, m_B is the mass of boron in solution at time t, f_B is the mass fraction of B in the glass, ρ is the density of the glass, and r_o is the initial radius of the glass spheres. We have calculated S_t with the final surface area to

obtain the maximum decrease in surface area over the test duration and to calculate an upper limit for the dissolution rate. The lower limit of the dissolution rate is calculated with the initial surface area. The values of NL(B) for tests with SRL EA, SRL 131A, and SRL 202A glasses conducted with -100 +200 mesh glass at 20,000 m^{-1} and at 90°C that were calculated with the initial surface area and the final surface area are plotted in Fig. 1. The values of NL(B) calculated with the final surface area–$NL(B)_{final}$–are greater than the values calculated with the initial surface area–$NL(B)_{initial}$–because the final surface area is less than the initial surface area. The upward curvature of the data (particular for the EA glass) is due to the decreasing surface area and does not indicate an increase in the glass dissolution rate.

Analcime and other mineral alteration phases formed within 22 days in tests conducted with SRL EA glass and within 182 days and 364 days in tests with SRL 131A and SRL 202A glasses. Lines in Fig. 1 show the dissolution rates for the three glasses immediately after these phases formed. These lines were drawn through the average of $NL(B)_{initial}$ and $NL(B)_{final}$ in the two tests after the phases had formed for all glasses, except the line for tests with the SRL EA glass. For this glass, the line was drawn through the origin and the average value of NL(B) from the 56-day test. The averages of $NL(B)_{initial}$ and $NL(B)_{final}$ were used because these values better represent the surface area of the glass *during* the test than either the initial or final surface area. The slope of the line for each glass gives what is referred to as the limiting rate. The limiting rates are about 0.22, 0.068, and 0.035 g/(m^2•d) for the SRL EA, SRL 131A, and SRL 202A glasses, respectively. These rates were used to calculate the rate at which the radius of the spherical particles decreases, which is defined as k=dr/dt, by dividing the limiting rates by the density of the glass, which is assumed to be 2.7 g/cm^3 for these three glasses. The rates extracted from the results of tests with several DWPF reference glasses in EJ-13 water at 90°C are summarized in Table III. We emphasize that the glass dissolves at this rate only after rate-affecting alteration phases have formed. An analytical expression relating the mass of glass that has dissolved with the remaining surface area can be written based on the geometry of shrinking spherical particles. In this approximation, the mass of glass that dissolves is simply the density of the glass times the loss of volume of the sphere as the radius decreases over time. The decrease in the volume can then be related to the decrease in surface area through the radius of the sphere. The geometric relationship between the mass of glass dissolved, the remaining surface area, and the dissolution rate can be written as

$$NL(B)(t) = \frac{M(t)}{S(t)} = \left(\frac{\rho k t'}{3}\right)\left\{1 + \frac{2 - \left(\frac{kt'}{R_p}\right)}{\left(1 - \frac{kt'}{R_p}\right)^2}\right\} + X \qquad (4)$$

where M(t) is the total mass of glass dissolved through time t, S(t) is the surface area that remains at time t, ρ is the glass density, k is the rate at which the radius of the spheres decrease, and R_p is the radius of the spheres when rate-affecting alteration phases first form. The term X represents glass dissolution that occurred *before* rate-affecting alteration phases formed; its form is identical to the first term, but with a dissolution constant different than k. The contribution of the X term to long-term dissolution is negligible after rate-affecting alteration phases form, and is not further considered here. We emphasize that the first term on the right hand side of Eq. 4 applies to corrosion *after* rate-affecting alteration phases have formed by using t', which is the time after those phases have formed. Since M(t) increases as S(t) decreases, the curve described by Eq. 4 curves upward as time increases. This does not mean that the dissolution rate increases with time.

To better show the common corrosion behavior of these glasses, and because of the small number of tests with any single glass in the presence of alteration phases, the data for several glasses is normalized as follows so data for the three glasses could be presented on a single plot. The time τ that is required for the glass to completely dissolve after alteration phases form is defined as $\tau = R_p/k$. The reaction time is scaled by τ to generate a dimensionless time variable, t_R, as $t_R = t'/\tau$; the value of t_R is 1 when the glass is completely dissolved. Similarly, the amount of

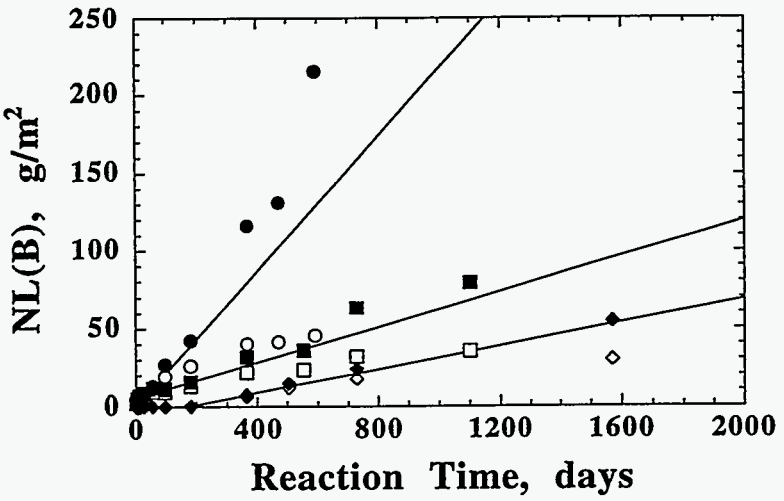

Figure 1. NL(B) for Tests at 20,000 m^{-1} with SRL EA glass (●), SRL 131A glass (■), and SRL 202A glass (◆). Open symbols calculated with initial surface area, filled symbols calculated with surface area remaining at the end of the test. Lines show the estimated dissolution rate for each glass (see text).

Table III. Dissolution Rates and pH Values Attained After Alteration Phases Form in Tests with Various DWPF Glasses

Glass	S/V, m^{-1}	t_p, d[a]	R_p, μm[b]	k, nm/d
SRL 131A	20,000	98	50	25
SRL 202A	20,000	182	56	13
SRL EA	20,000	0	56	82

[a]Test duration prior to formation of rate-affecting phases.
[b]Estimated grain size at t_p.

glass dissolved per unit area is normalized to a dimensionless quantity M_R, as $M_R = \{M(t)/S(t)\}/\{\rho \cdot R_p\}$. The values of k, t_p and R_p for tests with SRL EA, SRL 131, and SRL 202 glasses conducted at 20,000 m^{-1} are included in Table III. By substituting these dimensionless quantities, Eq. 4 transforms to

$$M_R = \left(\frac{t_R}{3}\right)\left(1+\frac{(2-t_R)}{(1-t_R)^2}\right) \qquad (5)$$

This gives a universal relationship between the mass measured in solution and the extent to which a glass dissolves if the radius of the glass particles decreases at a constant rate. The plot of M_R vs. t_R is shown in Fig. 2 along with the experimental results that have been transformed into reduced coordinates by dividing $NL(B)_{final}$ by the quantity ρR_p and scaling the test time as $t_R = (t-t_p)\cdot k/R_p$.

Average values of duplicate tests are plotted in Fig. 2 for clarity. After the differences in the values of k and t_p for the different glasses are taken into account, all three glasses show essentially the same behavior. The experimental values agree with the theoretical curve for reduced times less than about 0.3, but data from tests in which the extent of corrosion has progressed further (i.e., those data at t_R>0.3) clearly fall below the curve. Tests with SRL EA glass have the greatest extent of corrosion and show the deviation most clearly, while tests with SRL 202 show only a small deviation at the longest reaction time. Note that the deviation from the curve does *not*

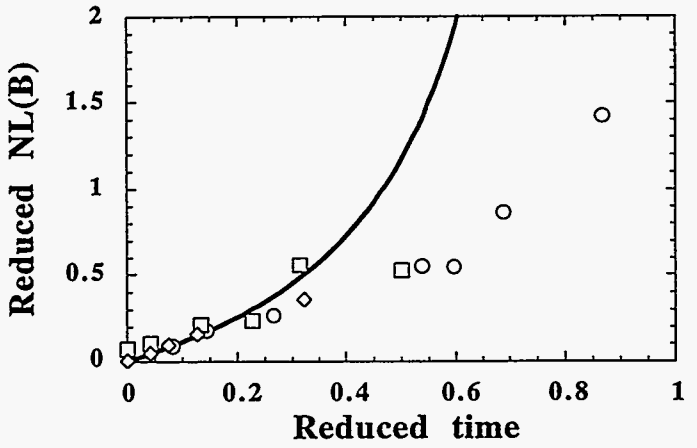

Figure 2. Theoretical Curve and Results of Tests at 20,000 m^{-1} with SRL EA (○), SRL 131A (□), and SRL 202A glass (◊), in Dimensionless Reduced Units.

correspond with the formation of the alteration phases, which occurs at $t_R = 0$ for all glasses. Neither is the deviation a result of using the final surface area of the glass in the calculations, since both M_R and the data are calculated with the final surface area.

The observation that the data follow the curve soon after rate-affecting phases form, while data from more advanced tests do not, indicates that glass corrosion cannot be modeled with a single rate constant or by a single mechanism. This suggests that the glass dissolution rate becomes moderated by another process after extended time periods (i.e., for t_R>0.3) that is not taken into account in Eq. 1. This other process may be associated with the glass, the solution, or the alteration phases. Alteration layers are known to form on the surface of the glass particles as the glass corrodes, and the thickness of the layer increases with the extent of corrosion. However, these layers are very porous and probably ineffective diffusion barriers [2, 3].

In these PCTs, the crushed glass settles at the bottom of the vessel and is covered by a 2-3 cm layer of water in tests at 20,000 m^{-1}. Precipitated phases are generally observed to form as a layer of sediment on top of the glass, which suggests that most precipitates form in the bulk solution and not within the solution between the glass grains. Diffusion of material from the glass to the bulk solution may affect the rate at long times. Because of differences in the compositions of the glass and of the suite of alteration phases, the solution will become depleted of some components needed to form alteration phases over time. This may slow the formation of some phases and limit their abundance, and may result in a slowing of glass dissolution. For example, based on the Na:Al:Si ratios of these glasses, the formation of zeolite alteration phases will be limited by the amount of Al. Hence, the solution concentration of Al will eventually become low enough to limit the formation of these phases.

The impact of other assumptions made in the present analysis on these results must be further evaluated, such as assumption of spherical particles and the assumption that B released from the glass is completely dissolved. Incorporation of small amounts of B into alteration phases would result in an apparent decrease in the dissolution rate. The significant change in the relative amounts of glass and alteration phases that occurs as the test proceeds may also affect the dissolution rate of the glass. Clearly, more work is needed to elucidate phenomena that affect the long-term corrosion behavior of waste glasses.

Regardless of the cause for the difference between the measured and predicted extents of dissolution that are plotted in Fig. 2, that predicted with a linear dissolution rate (the solid curve) does provide an upper limit for the measured extents of dissolution over long test durations. The long-term dissolution rates of these glasses at 90°C in solutions with pH values near 12 are: . 0.05 g/(m^2•d) for SRL 131 frit-based glasses, 0.04 g/(m^2•d) for SRL 202 frit-based glasses, and 0.2 g/(m^2•d) for the EA glass. Finally, based on Eq. 2, the glass dissolution rates will depend on the pH. The rates that were extracted in this paper are only relevant at pH values near 12. Tests conducted at lower S/V usually result in leachate solutions with lower pH values than tests at

20,000 m^{-1}. A few very long term tests are in progress at 2000 m^{-1} that may provide dissolution rates at lower pH values that can be compared to those discussed in this paper.

CONCLUSIONS

Corrosion of DWPF glasses in some laboratory tests results in the generation of highly concentrated solutions and the formation of alteration phases with a concomitant increase in the dissolution rate. The decrease in the surface area of the glass particles that occurs when the dissolution rate increases complicates the calculation of the dissolution rate. By modeling the glass particles as spheres, we have shown that dissolution is consistent with a constant decrease in the radius soon after certain phases form but not at long test durations. This may indicate that the precipitation rate of the alteration phases is limiting the dissolution rate of the glass, and that the expression currently used to calculate long-term glass behavior must be modified to accurately model long-term performance. Further testing is required to identify the cause of the effect and to assess its possible impact on the long-term corrosion behavior in a disposal site. Regardless, the present analysis suggests that the rate measured soon after alteration phases form probably provides an upper bound to the long-term dissolution rate.

ACKNOWLEDGMENTS

Work supported by the U.S. Department of Energy, Office of Environmental Management, under contract W-31-109-ENG-38.

REFERENCES

1. K. Lemmens and P. Van Isegham, Mater. Res. Soc. Symp. Proc. 257, 49-56 (1992).
2. X. Feng, J. K. Bates, E. C. Buck, C. R. Bradley, and M. Gong, Nucl. Technol. 104(2), 193-206 (1993).
3. W. L. Ebert, J. K. Bates, E. C. Buck, and C. R. Bradley, Mater. Res. Soc. Symp. Proc. 294, 569-576 (1993).
4. W.L. Ebert, A.J. Bakel, and N. R. Brown, in Proceedings International Topical Meeting on Nuclear and Hazardous Waste Management, Spectrum '96, Seattle, WA, August 18-23, 1996, pp. 569-575 (1996).
5. B. Grambow, *Nuclear Waste Glass Dissolution: Mechanism, Model, and Application*, JSS Report 87-02 (1987).
6. T. Advocat, J.L. Crovisier, B. Fritz, and E. Vernaz, Mater. Res. Soc. Symp. Proc. 176, 241-248 (1990).
7. D. M. Strachan, W. L. Bourcier, and B. P. McGrail, Radioactive Waste Management and Environmental Restoration 19, 129-145 (1994).
8. P. Van Iseghem and B. Grambow, Mater. Res. Soc. Symp. Proc. 112, 631-639 (1988).
9. W. L. Ebert, J. K. Bates, C. R. Bradley, E. C. Buck, N. L. Dietz, and N. R. Brown, Ceram. Trans. 39, 333-340 (1993).
10. X. Feng, Mater. Res. Soc. Symp. Proc. 333, 55-68 (1994).
11. J. K. Bates, W. L. Ebert, J. J. Mazer, J. P. Bradley, C. R. Bradley, and N. L. Dietz, Mater. Res. Soc. Symp. Proc. 212, 77-87 (1991).
12. J. K. Bates and M. J. Steindler, Mater. Res. Soc. Symp. Proc. 15, 83-90 (1983).
13. A. J. Bakel, W. L. Ebert, and J. S. Luo, Ceram. Trans. 61, 515-522 (1995).
14. B. P. McGrail and D. K. Peeler, *Evaluation of the Single-Pass Flow-Through Test to Support a Low-Activity Waste Specification*, Pacific Northwest Laboratory Report PNL-10746 (1995).
15. W. L. Bourcier, S. A. Carroll, and B. L. Phillips, Mater. Res. Soc. Symp. Proc. 333, 507-512 (1994).
16. K. G. Knauss, W. L. Bourcier, K. D. McKeegan, C. I. Merzbacher, S. N. Nguyen, F. J. Ryerson, D. K. Smith, and H. C. Weed, Mater. Res. Soc. Symp. Proc. 176, 371-381 (1990).
17. W. L. Ebert, and J. K. Bates, Nuclear Technol. 104(3), 372-384 (1993).
18. J. K. Bates, et al., *ANL Technical Support Program for DOE Environmental Restoration and Waste Management. Annual Report October 1993-September 1994*, Argonne National Laboratory Report ANL-95/20 (1995).